2020 IEEE International Conference on Systems, Man, and Cybernetics (SMC)
October 11-14, 2020. Toronto, Canada

A Static Gait Generation for Quadruped Robots with Optimized Walking Speed*

Yaqi Wang, Linqi Ye, Xueqian Wang, Nong Cheng, Houde Liu, and Bin Liang

Abstract—**Traversing at a high speed while maintaining stability is important for the application of quadruped robots. Prior works mainly concentrated on optimizing the stability margin of quadruped robots when walking through a variety of terrains. However, the problem of improving quadruped robots' walking velocity with static gait is less concerned in their works. In this paper, the static gait planning problem is considered under the assumption that a set of irregular footholds on the rough terrain is given, and two approaches are proposed to improve the walking speed. The first one is a distance optimization algorithm, which can minimize the moving distance of the center of gravity (COG) in the stance phases based on the stability and the kinematic constraint. The other is a velocity optimization algorithm, which enables the body and the feet to move at the highest velocity with the joint angular velocity limit. The joint application of these two optimization algorithms significantly improves the walking speed of the quadruped robot. Simulation results in V-REP are presented to demonstrate the effectiveness of the proposed approaches in improving the walking speed. Compared with the traditional gait planning techniques, one that moves the robot with the optimal stability margin, and the other that moves the robot without optimizing the velocity, our algorithms increase the average walking velocity by 81.6% and 32.8%, respectively.**

I. Introduction

Legged robots have attracted considerable interests in recent years with their potential to traverse a much wider variety of terrains than the traditional wheel or track-based robots. Among all the legged robots, such as biped, quadruped, and hexapod robots, quadruped robots have sparked more researches due to their superior ability to balance stability and complexity. For quadruped robots, gait planning is one of the most important topics among all the research areas since robust gait planning is a key aspect to control the robot to traverse different terrains efficiently and stably, especially for rough terrains with forbidden areas.

Corresponding author: Xueqian Wang.

*This work was supported by National Natural Science Foundation of China (61803221 & U1813216), Guangdong Young Talent with Scientific and Technological Innovation (2019TQ05Z111), and the Interdisciplinary Research Project of Graduate School of Shenzhen of Tsinghua University (JC2017005).

Y. Wang, L. Ye, X. Wang, and H. Liu are with the Center for Artificial Intelligence and Robotics, Graduate School at Shenzhen, Tsinghua University, 518055 Shenzhen, China (e-mail: yq-wang19@mails.tsinghua.edu.cn, {ye.linqi, wang.xq, liu,hd}@sz.tsinghua.edu.cn).

B. Liang, N. Cheng is with the Navigation and Control Research Center, Department of Automation, Tsinghua University, 100084 Beijing, China (e-mail: { bliang, ncheng } @tsinghua.edu.cn).

Before the gait planning, the gait type needs to be determined according to terrain conditions and gait features. In static gaits, at least three legs are in contact with the ground, which can increase the walking stability and is easier to be performed. These features are significant for real machines to traverse rough terrains. In free gaits, the body motion is planned as a function of the terrain condition and the robot state. Hence, free gaits offer better environment adaptability and facilitate path tracking. In this paper, static and free gaits for quadruped robots are selected since the test cases are built upon rough terrain with forbidden areas.

Walking stability is the basic requirement for gait planning, hence, various stability criteria were proposed to ensure stability. The concept of static stability was first defined by McGhee and Frank in [1], which indicates that the walking robot is statically stable if the vertical projection of the COG lies inside the support polygon. After that, many other stability criteria for the static gait were proposed, such as the Static Stability Margin (SSM) [2], the Longitudinal Stability Margin (LSM) [3], the Energy Stability Margin (ESM) [4] and the Normalized Energy Stability Margin (NESM) [5].

The gait planning with the stability constraint can guarantee that the robots traverse a flat terrain. However, if the quadruped robots want to traverse the rough terrains, footholds must be determined before planning the COG trajectory. In [6], a hierarchical strategy was proposed to plan the body movements with the optimal stability margin under the assumption that a set of irregular footholds are given. In [7], instead of pre-defining feasible footholds according to the terrain conditions, researchers first classified all the given points on the terrain as acceptable or unacceptable, and then selected a point from the acceptable terrain that was farthest from the current foothold and under the kinematic constraint. When the footholds were determined, all valid body configurations for the next footstep could then be calculated. In [8], three constraints were proposed to find valid body configurations.

After determining the valid body configurations, many approaches were proposed to plan the COG trajectory and most of them focus on improving the stability margin by adjusting the COG position. In [9], a posture adjustment strategy was proposed based on the potential energy to regulate the COG trajectory. In [10], two sway motions including a Y-Sway and E-Sway were proposed to increase the stability margin of the robot. In [11], a crawling gait was proposed based on the centroid trajectory.

However, none of the above works have considered improving the forward walking velocity of quadruped robots

978-1-7281-8526-2/20/$31.00 ©2020 IEEE

with static gait. To increase the locomotion speed of the robot, J. Zico Kolter introduced the double support triangle (DST) theory and decreased the adjustment processes of the COG in one crawl gait cycle from four to two in [12,13]. Bin Li proposed an optimized strategy that divides the adjustment of the COG into two types to improve the traversing velocity in [14]. These works partly address the slow movement problem of the quadruped robots with static gait. However, they only consider improving the walking speed by optimizing the COG trajectory.

In this paper, we take a further step to optimize both the COG trajectory and the velocities of the body and the feet. Two algorithms are proposed to increase the forward walking speed. In the first algorithm, the COG trajectory is optimized by setting the shortest COG moving distance as the optimization goal during each stance phase. In this process, checking where the COG can move is not simple, since the feasible areas of the COG need to satisfy both the stability constraint and the kinematic restriction. In the second algorithm, by solving the velocity optimization problems under the joint angular velocity constraint, the highest locomotion speeds of both the body and the feet can be obtained. The proposed methods have been tested on a quadruped robot in the V-REP simulation environment, and the simulation results demonstrate the improvement in forward walking speed compared to previous static gait planning methods.

In summary, The main contributions of this paper are three-fold:

(1) Compared to the prior arts on static gait planning over the rough terrains that are mainly concentrated on moving the robots with the optimal stability margin, our work improves the walking speed significantly while still achieving favorable static stability, which exhibits higher application potential.

(2) Two optimization algorithms, including the COG moving distance optimization and the velocity optimization, are jointly applied for the first time, which greatly address the problem of slow static movement of quadruped robots.

(3) Compared with the traditional static gait planning techniques, one that moves the robot with the optimal stability margin, and the other that moves the robot without optimizing the velocity, our algorithms significantly increase the walking velocity. It is remarked that the model is constructed according to a real quadruped robot that was developed at our laboratory.

The rest of this paper is organized as follows: Section II contains a simulation quadruped model and preliminaries. Section III describes the distance optimization algorithm, which minimizes the COG moving distance in the stance phases. Section IV introduces the velocity optimization method, which maximizes the body and the foot velocities with the limited joint angular velocity. Section V presents the simulation results. Section VI contains some conclusions.

II. Model and Preliminaries

A. The Simulation Model

The quadruped robot used in this paper to evaluate the proposed methods is shown in Fig. 1, which is constructed based on a real quadruped robot developed at our laboratory, as shown in Fig. 2. Each leg of the robots has three degrees of freedom with a roll-pitch-pitch type, and each leg contains two segments, an upper and a lower segment. The upper leg is connected to the body with a hip roll joint for sidestepping movement and a hip pitch joint for forward/backward movement. The lower leg is linked to the upper leg with a knee pitch joint for forward/backward movement. The mechanical parameters of the quadruped robot are listed in Table I.

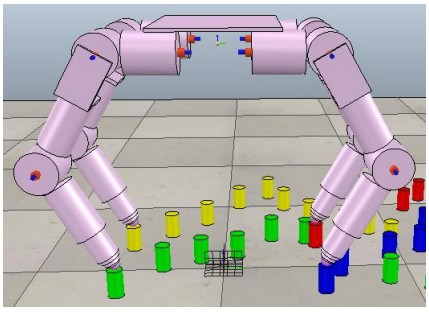

Fig. 1. The simulation quadruped robot.

Fig. 2. The prototype quadruped robot.

Table I. Mechanical Parameters of the Simulation Quadruped Robot

Body length	0.40 m
Body width	0.30 m
Body height	0.58 m
Upper leg length	0.30 m
Lower leg length	0.27 m
Total mass	25 kg
Maximum joint angular velocity	17 deg/s

B. Test Terrain

In this paper, we assume that the terrain information is already known, and a set of footholds has been pre-selected according to it. When walking on the rough terrain with many forbidden areas, it is indispensable for the quadruped robot to precisely step on the desired footholds. For simplicity and without loss of generality, it is assumed that the available footholds are constrained on a set of randomly distributed columns. As depicted in Fig. 3, there are 17×4 columns scattered randomly along an S-shape, which represents 17×4 locations of pre-selected footholds. Among them, the green, blue, yellow, and red columns represent the footholds for the right hind, right front, left hind, and left front foot, respectively. The column diameter is 4 cm and the column heights are the same. The scenario setting can roughly represent a real situation when the robot traverses rough terrain with forbidden areas. In this

case, the quadruped robot needs to use free gaits and constantly adjusts the COG trajectory to adapt to the given footholds.

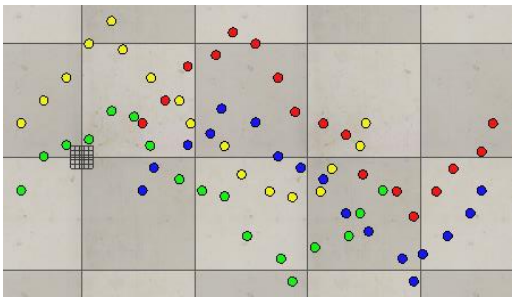

Fig. 3. The test terrain with a set of pre-selected footholds.

C. Assumptions

As a preliminary of the static gait planning, the following assumptions are made:

(1) It is assumed that the body of the quadruped robot keeps at a constant height during the locomotion due to the relatively low joint angular speed.

(2) It is assumed that the COG is located in the geometric center of the body since the leg configuration is symmetric.

(3) For simplicity, it is assumed that all the given footholds on the columns are in the same level plane.

D. The Leg Sequence and the Gait Cycle

There are eight phases in one gait cycle, which contains four stance phases and four leg swing phases. In the stance phases, the body is supported by four feet, and the COG is moving from the current position to the next optimized position. In the leg swing phases, one of the feet is swinging to its goal foothold, and the body is supported by the other three feet. Among all the six possible leg sequences for the static gait, we choose the sequence [right hind, right front, left hind, left front] (RH, RF, LH, LF) in this paper, which can provide the optimum static stability margin [3]. Correspondingly, name the swing phases of each leg as RH_SW, RF_SW, LH_SW, and LF_SW, and name four stance phases as COG_RH, COG_RF, COG_LH, COG_LF, then one gait cycle can be shown in Fig. 4.

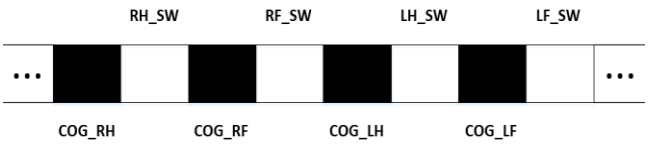

Fig. 4. One gait cycle of the static gait planning.

E. The Trajectory of the Swing Foot

In this paper, a box pattern trajectory is adopted to plan the swing foot trajectory, where the length of the trajectory is equal to the distance between the current foothold and the next foothold of the swing leg, and the height of the trajectory is a fixed value of 7 cm. This trajectory is shown in Fig. 5.

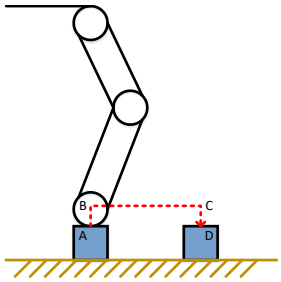

Fig. 5. The trajectory of the swing foot.

III. Optimization of the COG Trajectory

In this paper, our goal is to improve the walking velocity. To this end, the first approach we adopt is to reduce the COG moving distance during the stance phases. In order to find the shortest COG trajectory, we first define the feasible area based on the stability constraint and the kinematic limit where the body of the robot can move. We then choose an optimized position in this area as the desired vertical projection of the COG. In the following, we will introduce the stability constraint and the kinematic limit to define this feasible area and present the distance optimization problem.

A. The Stability Constraint

In static gait, whether the vertical projection of the COG lies inside the support polygon decides the stability of the quadruped robot. It is easy to prove that this condition can always hold in the stance phases, therefore only the leg swing phases with three support legs need to be considered. Then the static stability criterion can be represented as whether the projection of the COG lies inside the support triangle during the leg swing phases. To handle the inaccuracies in the measurement and increase the robustness to slight disturbance, a shrunken triangle with a given stability margin is defined inside the support triangle. This shrunken triangle is shown in Fig. 6, where O denotes the projection of the COG on the support plane at the beginning of the stance phase, O' denotes the desired projection of the COG on the support plane at the end of the stance phase, S_0 denotes the fixed margin, L_{ij} denotes the line joining two neighboring footholds of the i-th leg and the j-th leg, S_{ij} denotes the distance from O' to L_{ij}. Then the static stability criteria for the quadruped robots can be represented by:

$$S_{ij} \geq S_0,\ i,j \in \mathrm{A}_1,\mathrm{A}_2,\mathrm{A}_3,\mathrm{A}_4 \ and\ i \neq j, \tag{1}$$

where $\mathrm{A}_1=\{1,2,3\},\mathrm{A}_2=\{1,2,4\},\mathrm{A}_3=\{1,3,4\},\mathrm{A}_4=\{2,3,4\}$.

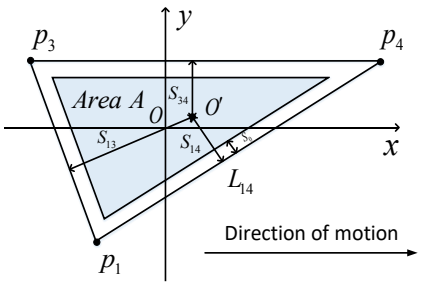

Fig. 6. The shrunken support triangle of the quadruped robot.

Let O be the origin of the coordinate, the axis x points to the moving direction, the axis y points from the right to the left, $p_i(x_i, y_i),\ (i \in \{1,2,3,4\})$ be the position of the i-th leg's foothold in the stance phase, then the line L_{ij} can be expressed as:

$$A_{ij}x + B_{ij}y + C_{ij} = 0, \tag{2}$$

where $A_{ij} = y_i - y_j$, $B_{ij} = x_j - x_i$, and $C_{ij} = x_i(y_j - y_i) + y_i(x_i - x_j)$.

Let $p'_o(x'_o, y'_o)$ be the position of O', then the distance S_{ij} can be expressed as:

$$S_{\mathrm{ij}} = \frac{\left|A_{ij}x'_0 + B_{ij}y'_0 + C_{ij}\right|}{\sqrt{A_{ij}^{\ 2} + B_{ij}^{\ 2}}}. \tag{3}$$

Denote the feasible area for the vertical projection of the COG that satisfies the stability constraints as Area A. Assume that the subscript i is smaller than the subscript j, Area A can be calculated by combing Eq. (1) and Eq. (3):

$$\mu\frac{A_{ij}x'_0 + B_{ij}y'_0 + C_{ij}}{\sqrt{A_{ij}^{\ 2} + B_{ij}^{\ 2}}} \geq S_0,\ \ \mu = \begin{cases} +1, & if\ i=1, j=2. \\ -1, & if\ i=3, j=4. \end{cases} \tag{4}$$

$$\begin{cases} \mu\dfrac{A_{ij}x'_0 + B_{ij}y'_0 + C_{ij}}{\sqrt{A_{ij}^{\ 2} + B_{ij}^{\ 2}}} \geq S_0,\ x_i \geq x_j \\ -\mu\dfrac{A_{ij}x'_0 + B_{ij}y'_0 + C_{ij}}{\sqrt{A_{ij}^{\ 2} + B_{ij}^{\ 2}}} \geq S_0,\ x_i < x_j \end{cases},\ \mu = \begin{cases} +1, & if\ i=1, j=3. \\ -1, & if\ i=2, j=4. \end{cases} \tag{5}$$

$$\begin{cases} \dfrac{A_{14}x'_0 + B_{14}y'_0 + C_{14}}{\sqrt{A_{14}^{\ 2} + B_{14}^{\ 2}}} \geq S_0,\ if\ the\ swing\ leg\ is\ 2. \\ -\dfrac{A_{14}x'_0 + B_{14}y'_0 + C_{14}}{\sqrt{A_{14}^{\ 2} + B_{14}^{\ 2}}} \geq S_0,\ if\ the\ swing\ leg\ is\ 3. \end{cases} \tag{6}$$

$$\begin{cases} \dfrac{A_{23}x'_0 + B_{23}y'_0 + C_{23}}{\sqrt{A_{23}^{\ 2} + B_{23}^{\ 2}}} \geq S_0,\ if\ the\ swing\ leg\ is\ 1. \\ -\dfrac{A_{23}x'_0 + B_{23}y'_0 + C_{23}}{\sqrt{A_{23}^{\ 2} + B_{23}^{\ 2}}} \geq S_0,\ if\ the\ swing\ leg\ is\ 4. \end{cases} \tag{7}$$

B. The Kinematic Restriction

The kinematic restriction is another constraint on the robot caused by the limited workspace of each leg. The kinematic restriction affects the motion of the quadruped robot in two ways. In the stance phases, each leg's current foothold must be located in its reachable area. In the leg swing phases, the next foothold for the swing leg must be located in its reachable area.

To determine the position in the shrunken triangle that satisfies the kinematic constraint, we first calculate the reachable area of each leg in the support plane. Let the length of the upper leg be l_2, the length of the lower leg be l_3, the height of the body be h. Supposing that the movable range of three joint angles of each leg is $(0, 2\pi)$, it is easy to prove that the workspace of each leg is a sphere with a spherical center at the hip-roll-pitch joint intersection and with a radius of $l_2 + l_3$. Then we can conclude that the reachable area of each leg in the support plane is a circle with a center at the projection of the hip-roll-pitch joint intersection, and the radius of this circle can be calculated as follows:

$$r = \sqrt{(l_2 + l_3)^2 - h^2}. \tag{8}$$

Then, we can formulate the feasible area for the projection of the COG in the shrunken triangle that meets the kinematic limit. Denote this area as Area B, the length of the body as $2b$, and the width of the body as $2a$. As shown in Fig. 7, let $p_i(x_i, y_i),\ (i \in \{1,2,3,4\})$ be the position of the i-th leg's foothold in the stance phase, k be the sequence number of the swing leg in the next phase, $p'_k(x'_k, y'_k)$ be the position of the swing leg's foothold, then Area B can be expressed as:

$$\begin{aligned} &\left(x_i - \left(x'_o + \alpha b\right)\right)^2 + \left(y_i - \left(y'_o + \beta a\right)\right)^2 \leq r^2, \\ &\left(x'_k - \left(x'_o + \alpha b\right)\right)^2 + \left(y'_k - \left(y'_o + \beta a\right)\right)^2 \leq r^2, \end{aligned} \tag{9}$$

where $\alpha = \begin{cases} 1, & if\ i,k=2,4 \\ -1, & if\ i,k=1,3 \end{cases}$, $\beta = \begin{cases} 1, & if\ i,k=3,4 \\ -1, & if\ i,k=1,2 \end{cases}$.

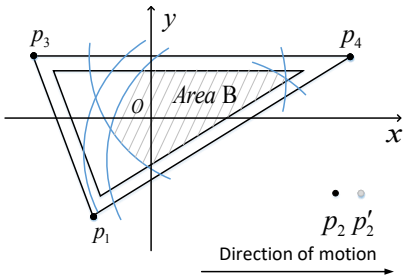

Fig. 7. The feasible area of the COG projection with the kinematic limit, in which the arcs are the boundaries of the reachable area of the legs.

C. The Distance Optimization Problem

In section II-B, the feasible area of the projection of the COG has been determined. In this section, a distance optimization algorithm will be presented to calculate a point in this area, which meets the condition that the distance from the projection of the COG at the beginning of the stance phase to this point is the shortest. Since the shortest distance between two points is a straight line, we let the COG moves along a straight line during each stance phase.

Let $p_o(x_o, y_o)$ be the position of the initial projection of the COG, $p'_o(x'_o, y'_o)$ be the position of the desired projection of the COG, d be the distance from $p_o(x_o, y_o)$ to $p'_o(x'_o, y'_o)$. We select the COG moving distance during one stance phase as the cost function, then the distance optimization problem can be expressed as:

$$\begin{aligned} \min\quad & d = \left|p_o' - p_o\right| \\ \text{s.t.}\quad & p'_o \in Area\ \mathrm{A} \bigcup Area\ \mathrm{B}. \end{aligned} \tag{10}$$

By solving the optimization problem defined above, the target position for the COG with the minimal travel distance can be found during each stance phase. Since there are four stance phases in one gait cycle, the optimization calculation is performed four times in a cycle.

IV. Optimization of the Velocity

In this section, the velocity optimization algorithms are proposed to increase the walking velocity. With the limitation on the joint angular velocity, the optimization algorithms can calculate the maximum foot velocity and the maximum body velocity.

A. The Maximum Foot Velocity

To calculate the maximum foot velocity with the restriction on the joint angular velocity, firstly, we need to derive the relationship between the foot velocity and the three joint angular velocities of the leg. Secondly, to guarantee that the foot moves along the desired trajectory, the three components of the foot velocity need to satisfy some restrictions. Then based on these restrictions, the proportional relationships of the three joint angular velocities can be constructed. When the foot moves at the maximum speed, there must be a joint with the maximum angular velocity. However, we cannot determine in advance which joint has the maximum angular velocity. Hence, an algorithm is proposed to determine which joint has the maximum joint angular velocity. Finally, according to the relationship derived in the first step, the maximum foot speed can be obtained.

1. Relationship between the foot velocity and the three joint angular velocities. It can be easily proven that the relationships between the foot velocity and the three joint angular velocities for Leg 1 and Leg 3 are the same, and the same is true for Leg 2 and Leg 4 due to the symmetric configuration. Therefore, we take Leg 1 and Leg 2 as examples to analyze the relationships. As shown in Fig. 8, the origin of the coordinate frame $\{O_b\}$ is established in the center of the body, the x axis points to the forward direction, the y axis points from the right to the left, the z axis points in the opposite direction of the direction of gravity, and four fixed coordinate frames $\{O_{i0}\},(i=1,2,3,4)$ are established in the center of four hip-roll joints. Based on the D-H rules, the coordinate frames $\{O_{i1}\},\{O_{i2}\},\{O_{i3}\}$ are located at the center of four hip-roll joints, hip-pitch joints, and knee-pitch joints respectively.

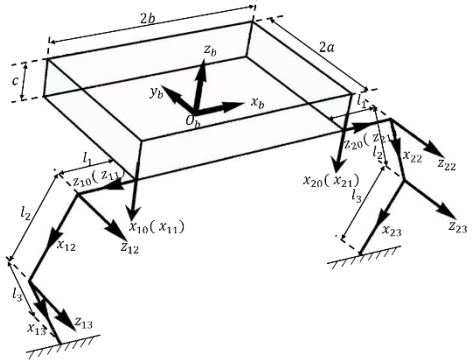

Fig. 8. D-H coordinate frames of the quadruped robots.

Let $P_i(x_i,y_i,z_i)$ be the position of the foothold of the i-th leg in the coordinate frame $\{O_b\}$, $v_i(v_{ix},v_{iy},v_{iz})$ be the foot velocity of the i-th leg, θ_{ij} be the j-th joint angle of the i-th leg, w_{ij} be the j-th joint angular velocity of the i-th leg, then $P_i(x_i,y_i,z_i)$ can be written as the function of θ_{ij}:

$$P_i=\left[\lambda(l_2s_2-l_3s_3)+\alpha b, s_1(l_2c_2+l_3c_3)+\beta a, -c_1(l_2c_2+l_3c_3)\right], \quad (11)$$

where $\alpha=\begin{cases}1, & if\ i=2,4\\ -1, & if\ i=1,3\end{cases}$, $\beta=\begin{cases}1, & if\ i=3,4\\ -1, & if\ i=1,2\end{cases}$.

Differentiating Eq. (11), the relationships between $v_i(v_{ix},v_{iy},v_{iz})$ and w_{ij} are shown as follows:

$$\begin{aligned} v_{ix}&=\lambda(l_2w_{i2}c_2-l_3w_{i3}c_3),\\ v_{iy}&=w_{i1}c_1(l_2c_2+l_3c_3)-s_1(l_2w_{i2}s_2+l_3w_{i3}s_3),\\ v_{iz}&=w_{i1}s_1(l_2c_2+l_3c_3)+c_1(l_2w_{i2}s_2+l_3w_{i3}s_3), \end{aligned} \quad (12)$$

where $c_1=\cos(\theta_{i1})$, $s_1=\sin(\theta_{i1})$, $c_2=\cos(\theta_{i2})$, $s_2=\sin(\theta_{i2})$, $c_3=\cos(-\theta_{i3}-\theta_{i2})$, $s_3=\sin(-\theta_{i3}-\theta_{i2})$, $\lambda=\begin{cases}-1, & if\ i=1,3\\ +1, & if\ i=2,4\end{cases}$.

2. Relationships between the three joint angular velocities. As shown in fig. 5, in this paper, we move the feet in a box pattern. Denote AB and CD as the two vertical lines of the foot trajectory respectively, and the horizontal line as BC. To ensure that the foot can transfer along with the given trajectory AB and CD, the foot velocity needs to satisfy the condition that the foot velocity along both x axis and y axis is equal to zero, which can be expressed as:

$$\begin{aligned} &\lambda(l_2w_{i2}c_2-l_3w_{i3}c_3)=0,\\ &w_{i1}c_1(l_2c_2+l_3c_3)-s_1(l_2w_{i2}s_2+l_3w_{i3}s_3)=0. \end{aligned} \quad (13)$$

According to Eq. (13), the proportional relationship of three joint velocities can be solved as follows:

$$\begin{aligned} w_{i1}/w_{i2}&=\left(s_1l_2(c_2s_3+c_3s_2)\right)\Big/\left(c_1c_3(l_2c_2+l_3c_3)\right),\\ w_{i1}/w_{i3}&=\left(s_1l_2l_3(c_2s_3+c_3s_2)\right)\Big/\left(c_1(l_2c_2+l_3c_3)^2\right). \end{aligned} \quad (14)$$

To guarantee that the foot moves along the given trajectory BC, the foot velocity needs to satisfy the following conditions: 1) The foot speed along the z axis is equal to zero. 2) The ratio of the foot speed along the x axis to the foot speed along the y axis is equal to the slope of the trajectory BC. Denoting the slope of the trajectory BC as k, the condition can be expressed as:

$$\begin{aligned} &w_{i1}c_1(l_2c_2+l_3c_3)-s_1(l_2w_{i2}s_2+l_3w_{i3}s_3)=k\lambda(l_2w_{i2}c_2-l_3w_{i3}c_3),\\ &w_{i1}s_1(l_2c_2+l_3c_3)+c_1(l_2w_{i2}s_2+l_3w_{i3}s_3)=0. \end{aligned} \quad (15)$$

According to Eq. (15), the proportional relationship of three joint velocities can be represented as follows:

$$\begin{aligned} w_{i1}/w_{i2}&=-\left(c_1l_2k\lambda(c_2s_3+c_3s_2)\right)\Big/\left((l_2c_2+l_3c_3)(s_3c_1^2+s_3s_1^2-c_3s_1k\lambda)\right),\\ w_{i1}/w_{i3}&=c_1l_2l_3k\lambda(c_2s_3+c_3s_2)\Big/\left((l_2c_2+l_3c_3)(l_3s_3-l_2s_2-s_1k\lambda(l_2c_2+l_3c_3))\right). \end{aligned} \quad (16)$$

3. Algorithms of determining which joint has the maximum joint angular velocity. Based on the proportional relationships of the three joint angular velocities and the relationship between the foot velocity and three joint angular velocities, if we know which joint has the maximum angular

velocity, we can calculate the maximum foot velocity. However, it cannot be determined in advance which joint has the maximum angular velocity. Hence, we propose an algorithm to determine it. When the foot moves along the line BC, an overall scheme of the algorithm is shown in Fig. 9:

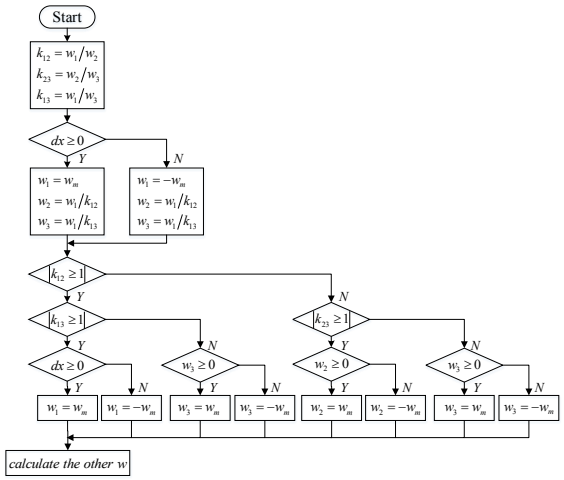

Fig. 9. The algorithm of determining which joint has the maximum joint angular velocity when the foot moves along the line BC.

When the foot moves along the line AB and CD, an overall scheme of the algorithm is shown in Fig. 10:

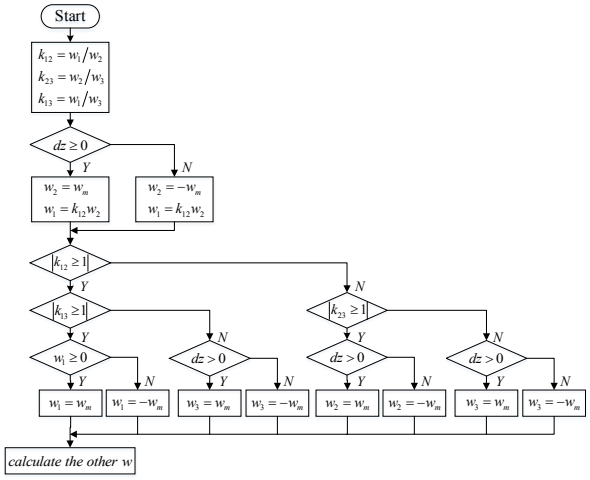

Fig. 10. The algorithm of determining which joint has the maximum joint angular velocity when the foot moves along the line AB and CD.

By the above algorithms, the three joint angular velocities can be calculated. Then, according to Eq. (12), the maximum foot velocity can be obtained.

B. The Maximum Body Velocity

In the stance phases, the feet are fixed and the body is moving. Since the relative speed of the body to the foot is opposite to the relative speed of the foot to the body, which has been calculated in Section IV-A. By using the algorithms derived in Section IV-A to each leg, four maximum velocities can be calculated. To ensure that each leg's joint angular velocities satisfy the joint angular velocity limit, the smallest value is selected from the four maximum velocities as the body's maximum moving speed.

V. SIMULATION RESULTS

A. Simulation Setup

To validate the efficiency of the proposed algorithms, simulations are implemented in the robot simulator V-REP with the Newton physical engine. The simulation quadruped robot is previously shown in Fig. 1. The maximum joint angular velocity of each joint is 17 degrees per second.

Unlike the quadruped robots in the previous papers, the simulation robot in this paper is constructed with the backward/forward leg configuration in consideration of the following reasons: 1) Since the leg is heavy with one motor placed on the knee, the symmetric configuration is adopted to ensure that the COG is close to the geometric center; 2) The backward/forward configuration can avoid collision between the front leg and the hind leg.

B. Simulation Results and Analysis

To demonstrate the advantages of our proposed static gait planning method, we compare the proposed method with two other static gait planning approaches. In one method, the robot moves with the optimal stability margin based on the SSM. In the other, only the COG moving distance is optimized without velocity optimization on the body and the feet. In the following, we will present and analyze the simulation results of these three gait planning methods.

1. The static gait planning method proposed in this paper. In this paper, two optimization algorithms are introduced to improve the walking velocity. One is the distance optimization algorithm, which optimizes the walking distance traveled by the COG. The other is the velocity optimization algorithm that computes the highest velocity of the body and the feet with the limited joint angular velocity. Fig. 11 shows the foot trajectory of the simulated quadruped robot that uses our proposed method to traverse the test terrain. Fig. 12 and Fig. 13 show some simulation curves of our proposed method.

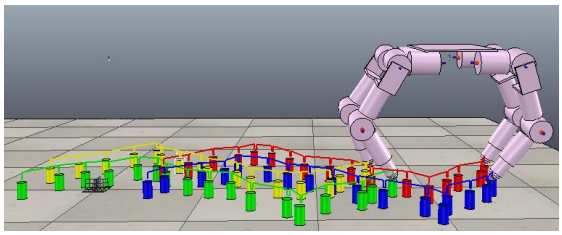

Fig. 11. The foot trajectory of the simulated quadruped robot.

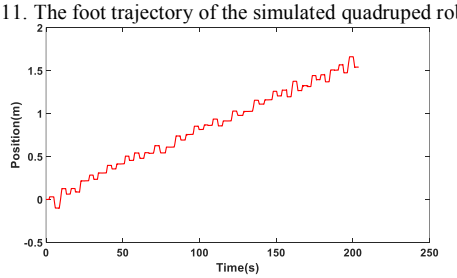

Fig. 12. The position variation curve of the COG along the forward direction for the proposed method.

As shown in Fig. 12, the horizontal axis represents the time, and the vertical axis represents the COG moving distance along the forward walking direction, which is the projection of the body position on x-axis in this article. It can be observed that it takes 205 seconds for the robot to walk from the start to the end. Since the distance along the forward walking direction from the start to the end is 1.5 m, the average forward walking velocity is 7.32 mm/s.

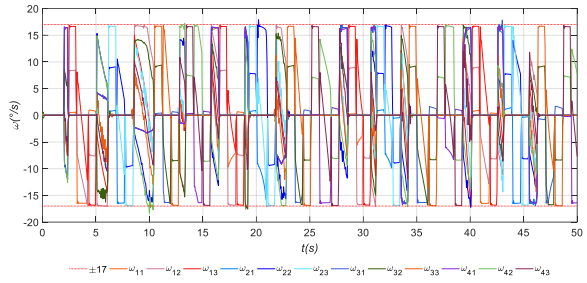

Fig. 13. The angular velocity variation curves of the joints.

As presented in Fig. 13, the horizontal axisf represents the time, and the vertical axis represents the joint angular velocities of all the twelve joints. It can be seen that all joint angular velocities satisfy the joint angular velocity limitation, which validates the effectiveness of the proposed velocity optimization algorithm.

2. The method based on the SSM. The difference between the method based on the SSM and the proposed method is the optimization goal. The method based on the SSM optimizes the COG position with the optimal stability margin. The simulation result is presented in Fig. 14.

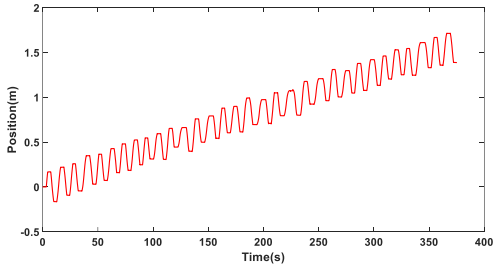

Fig. 14. The position variation curve of the COG along the forward direction for the method based on the SSM.

It can be observed from Fig. 14 that it takes 372 seconds for the robot to walk from the start to the end. Hence, the average walking velocity is 4.03 mm/s. Comparing the simulation results in Fig. 12 and Fig. 14, the proposed method costs less time than the approach based on the SSM due to the shorter COG moving distance. Hence, it can be concluded that our proposed method improves the walking velocity while keeping the static stability compared to the approach based on the SSM.

3. The method without optimizing the velocities. In the method that does not consider the speed optimization, the body and the feet move at a given speed of 5 mm/s and the joint angular velocities are limited in the simulation settings. The simulation result is shown in Fig. 15.

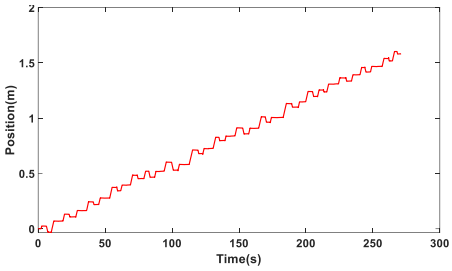

Fig. 15. The position variation curve of the COG along the forward direction for the method without velocity optimization.

From Fig. 15, we can see that it takes 272 seconds for the robot to walk from the start to the end. Hence, the average walking velocity is 5.51 mm/s. Comparing the simulation results in Fig. 12 and Fig. 15, it is obvious that the time taken by the robot with this method is longer than our proposed method. Hence, we can conclude that our proposed method can improve the walking velocity compared to the method without optimizing the velocity.

In order to present the relationships among these three static gait planning methods more clearly, we list the above simulation results in Table II, which shows the time spent on moving from the start to the end and the walking velocity of these three approaches.

Table II. SIMULATION RESULTS OF THE THREE STATIC GAIT PLANNING METHODS

	Time (s)	Velocity (mm/s)
Our proposed method	205	7.32
The method based on the SSM	372	4.03
The method without velocity optimization	272	5.51

As shown in Table II, our proposed method achieves considerable walking velocity improvement over the other two static gait planning methods, which are 81.6% compared to the method based on the SSM and 32.8% compared to the method without the velocity optimization, respectively.

VI. CONCLUSIONS

In this paper, we propose two optimization algorithms for the quadruped robot, which enable the robot to walk through a set of randomly distributed columns with improved walking velocity. The first one is the distance optimization algorithm, which reduces the COG moving distance in the stance phases based on the stability constraint and the kinematic limit. The other is the velocity optimization algorithm, which enables the body and the feet to move at the highest speed with the limited joint angular velocity. The joint application of these two algorithms has solved the slow movement problem of the quadruped robots with static gait. Simulation results show the effectiveness of the proposed methods.

This work has assumed that all the footholds are in the same plane. In the future, more complicated test terrains that contain the footholds with different heights will be considered. Furthermore, experiments will be done with our real robot.

REFERENCES

[1] R. B. McGhee and A. A. Frank, "On the stability properties of quadruped creeping gaits," *Mathematical Biosciences,* vol.3, (1968), pp.331-351.

[2] C. D. Zhang and S. M. Song, "Stability Analysis of Wave-Crab Gaits of a Quadruped," *Journal of Robotic Systems,* vol. 7, no. 2, pp. 243-276, Apr 1990.

[3] P. G. De Santos, E. Garcia, and J. Estremera, "Quadrupedal locomotion: An introduction to the control of four-legged robots," *Springer-Verlag London Limited,* 2006

[4] D. A. Messuri and C. A. Klein, "Automatic Body Regulation for Maintaining Stability of a Legged Vehicle During Rough-Terrain Locomotion," *IEEE Journal on Robotics and Automation,* Article vol. 1, no. 3, pp. 132-141, 1985.

[5] S. Hirose, H. Tsukagoshi, and K. Yoneda, "Normalized energy stability margin and its contour of walking vehicles on rough terrain," *Proceedings - IEEE International Conference on Robotics and Automation,* vol. 1, pp. 181-186, 2001.

[6] Y. J. Lee and Z. N. Bien, "A Hierarchical Strategy for Planning Crab Gaits of a Quadruped Walking Robot," *Robotica,* vol. 12, pp. 23-31, Jan-Feb 1994.

[7] J. R. Rebula, P. D. Neuhaus, B. V. Bonnlander, M. J. Johnson, and J. E. Pratt, "A controller for the LittleDog quadruped walking on rough terrain," *Proceedings of the 2007 IEEE International Conference on Robotics and Automation, vols 1-10,* pp. 1467-1473, 2007.

[8] V. G. Loc, I. M. Koo, D. T. Tran, S. Park, H. Moon, and H. R. Choi, "Body Workspace of Quadruped Walking Robot and its Applicability in Legged Locomotion," *Journal of Intelligent & Robotic Systems,* vol. 67, no. 3-4, pp. 271-284, Sep 2012.

[9] X. Shao, Y. Yang, Y. Zhang, and W. Wang, "Trajectory planning and posture adjustment of a quadruped robot for obstacle striding," *IEEE International Conference on Robotics and Biomimetics, ROBIO 2011,* pp. 1924-1929, 2011.

[10] F.-T. Cheng, H.-L. Lee, and D. E. Orin, "Increasing the locomotive stability margin of multilegged vehicles," *Proceedings - IEEE International Conference on Robotics and Automation,* Article vol. 3, pp. 1708-1714, 1999.

[11] B. H. Kim, "Centroid-based Analysis of Quadruped-Robot Walking Balance," *ICAR: 2009 14th International Conference on Advanced Robotics,* vols 1 and 2, pp. 354-359, 2009.

[12] J. Buchli, M. Kalakrishnan, M. Mistry, P. Pastor, and S. Schaal, "Compliant Quadruped Locomotion Over Rough Terrain," *IEEE-RSJ International Conference on Intelligent Robots and Systems,* pp. 814-820, 2009.

[13] J. Z. Kolter, M. R. Rodgers, and A. Y. Ng, "A control architecture for quadruped locomotion over rough terrain," *IEEE International Conference on Robotics and Automation,* vols 1-9, pp. 811-818, 2008.

[14] B. Li, Y. X. Xin, Y. B. Li, and X. W. Rong, "An Optimized Discontinuous Crawl Gait for Quadruped Robot," *Chinese Automation Congress (CAC),* pp. 266-271, 2017.